International Journal of Hydrogen Energy 105 (2025) 1309–1319

Contents lists available at ScienceDirect

International Journal of Hydrogen Energy

journal homepage: www.elsevier.com/locate/he

Exploring the environmental and economic benefits of hybrid natural gas and biomass conversion to liquid fuels

Mostafa Zarandi [a], Mehdi Panahi [b,*], Ahmad Rafiee [c], Sajad Namazi Rad [b], Ángel Galán-Martín [d], Josep M. Mateo-Sanz [a], Laureano Jiménez [a,**]

[a] Departament d'Enginyeria Química, Universitat Rovira i Virgili, Av. Paisos Catalans, 26, 43007 Tarragona, Spain
[b] Department of Chemical Engineering, Faculty of Engineering, Ferdowsi University of Mashhad, Mashhad, Iran
[c] Department of Mechanical and Biomedical Engineering, University of Galway, Ireland
[d] Department of Chemical, Environmental and Materials Engineering, Center for Advanced Studies in Earth Sciences, Energy and Environment (CEACTEMA), University of Jaén, Campus Las Lagunillas, 23071, Jaén, Spain

ARTICLE INFO

Handling Editor: Prof I Tolj

Keywords:
Fischer-tropsch
Techno-economic
Biomass to liquid
Natural gas to liquid
Life cycle assessment
Integration process

ABSTRACT

Liquid fuels as the primary global energy source will experience a demand peak in the near future. Fischer-Tropsch technology provides liquid fuels to fulfill part of this demand from a variety of carbon-rich materials. Biomass is a renewable source of carbon that complements conventional liquid fuels. The low efficiency of Biomass to Liquid (BtL) processes which roots to a deficiency of hydrogen in produced syngas makes this process less competitive. This work investigates the enhancement of the BtL process by the integration of rich hydrogen syngas from the Gas to Liquid (GtL) process. The rigorous techno-economic analysis demonstrates that the optimal mass blending ratio between the two feedstocks, biomass and natural gas, is 4.27 in the integrated process of natural gas-biomass to liquid fuels (GBtL). The life cycle assessment of the hybrid system highlights the impact of biomass feed on global warming by considering the biogenic carbon in the feedstock. The analysis reveals that a 30% alteration in biomass feedstock leads to approximately 30% variation in the global warming emission impact of the hybrid plant. Utilizing the different types of biomass feedstock is also evaluated and compared as a potential solution for the difficulties in the supply chain and defining the best type of biomass for the feedstock.

1. Introduction

The evolving landscape of the energy and transportation sectors, marked by the transition to renewable sources and the rising prices of fossil fuels stemming from the unstable socio-political situation, calls for more flexible technologies in the production of liquid fuels (LFs) [1].

LFs are versatile hydrocarbon-based substances that can be used in vehicles, heating systems, and for power generation. They are commonly produced from fossil resources such as petroleum, coal, and natural gas which are converted to gasoline, diesel, and jet fuel. Alternatively, their production from biomass resources is attracting increased attention to generate environmentally friendly biofuels like biodiesel, bioethanol, or biogas [2].

Fossil-based LFs currently dominate the global energy sector accounting for 30% of the energy supply but its consumption is expected to peak in the coming years. These fuels hold favored features due to current infrastructures and transportation technologies designed for LFs, and their high energy density [1,2].

Within the portfolio of options for LF production, Fischer-Tropsch (FT) synthesis stands out because it can utilize all carbon materials as potential feedstocks. In the FT process, the catalytic FT reactor is the core unit, where the syngas (a blend of CO and H_2) is converted into LFs which can later be upgraded and refined in downstream units. LFs obtained through the FT process possess desirable properties such as being sulfur-free, simplifying downstream processing [3]. The conversion of natural gas and coal to LFs (GtL and CtL, respectively) are more mature technology due to their high efficiency and low complexity compared to the conversion of biomass and power to LFs (BtL and PtL). However, the utilization of biomass as a feedstock has garnered attention within the scientific community due to the growing awareness of the need for more

* Corresponding author.
** Corresponding author.
E-mail addresses: mehdi.panahi@um.ac.ir (M. Panahi), laureano.jimenez@urv.cat (L. Jiménez).

https://doi.org/10.1016/j.ijhydene.2025.01.290
Received 13 June 2024; Received in revised form 22 November 2024; Accepted 18 January 2025
Available online 30 January 2025

eco-friendly fuels [4,5].

In a conventional biomass-to-liquid facility (BtL plant), the biomass is first subjected to grinding and drying processes to prepare the biomass for the gasification reactor [6]. Subsequently, the gasification reactor initiates a thermochemical transformation, converting the feedstock into syngas. Gasification has become a focus of attention due to the growing emphasis on environmentally friendly fuels.

The main challenge of the BtL plants is their relatively low process efficiency. The BtL conversion efficiency ranges from 28 to 40%, which means that approximately just one-third of the feedstock is converted into the desired product (LFs), while the remaining portion of the feedstock is converted into CO_2, burned as fuel to supply energy of the process or exits the process as waste [7]. Chiodini et al. highlighted the deficient H_2:CO ratio in the produced syngas [8]. The FT reactor operates effectively with an input mole ratio of hydrogen: carbon monoxide of 2:1 [9]. However, the gasified biomass contains a limited amount of H_2, necessitating compensation through a water gas shift (WGS) reactor. In the WGS reactor, carbon monoxide (CO) reacts with excess steam to produce H_2 and, inevitably, carbon dioxide (CO_2) [10]. Approaches included the use of Ni-based [11] alumina or silica-alumina catalysts impregnated with alkali [12]. An alternative solution involving the incorporation of a chemical looping design into the gasification process has been also explored [13].

The operational parameters during the gasification stage, including the amount of oxygen and steam utilized, play a pivotal role in increasing the H_2 yield [14,15]. Moreover, co-gasification of biomass and methane also has a substantial impact on the H_2 content within the syngas. Shen et al. (2018) demonstrated that adding methane to biomass in a reactor with Ni and alumina-based catalyst can increase the H_2/CO ratio to two [16]. Hence, the presence of methane in the gasification process plays a crucial role, as its addition limits the reverse steam methane reforming reaction, allowing the achievement of more than 80% mole fraction of H_2 in the gas output [17].

Another method to address the H_2 deficiency in syngas involves combining the gasification process with syngas enrichment from a GtL process. GtL plants employ different technologies for syngas production, such as auto-thermal reforming, steam methane reforming (SMR), and partial oxidation. Notably, the SMR process leads to the highest H_2/CO ratio and relatively lowest power requirement [9]. In this context, more than two decades ago, Brogwardt et al. (1997) proposed biomass gasification alongside the reforming of methane for methanol production; however, their study did not include the FT stage [18,19]. Nevertheless, the co-utilization of biomass and natural gas represents a great opportunity to efficiently utilize the carbon and hydrogen content of different feedstocks while preventing the conversion into CO_2 during the WGS process [20].

As for today, the large-scale deployment of the BtL plants in the landscape is limited due to several factors that hinder their economical implementation. Perhaps the main barrier is the relatively low efficiency and the economic feasibility due to capital investment. Hence, the integration of BtL with the GtL process holds promise in mitigating this economic drawback and improving the overall economic performance making it a more attractive option for pursuing sustainable and greener energy solutions [21]. Although conventional liquid fuel production still maintains the cost advantage, this gap is decreasing due to optimal process design and credit for environmental factors. Additionally, this integration presents an intriguing opportunity to leverage the economic advantages of GtL technology to reduce the production costs of the BtL plants. Another important barrier includes the technical complexity of exploiting the biomass resources available. Addressing the substantial challenge of supplying a large quantity of biomass feedstock sustainably is a critical aspect of this integration [22]. Hence, conducting an economic and environmental analysis can elucidate the benefits of this integration by considering various types of feedstocks.

Prior studies have demonstrated that hybridizing natural gas and biomass conversions to LFs (referred to as GBtL) has the potential to reduce greenhouse gas (GHG) emissions while maintaining economic competitiveness compared to the hybrid conversion of coal and biomass to liquid fuels (CBtL) [23]. GBtL systems can be economically competitive with fossil fuel-based processes while producing nearly half of GHG emissions [24]. Even achieving a net negative GHG emissions balance is possible by implementing carbon capture processes in both the GBtL and BtL plants. However, an increase in the natural gas portion in feedstock may lead to positive GHG from a life cycle perspective [25]. Hence, there is a compelling argument to limit the use of natural gas in line with the advanced biofuel standards [26].

Zhang et al. emphasized that co-processing natural gas with biomass in the GBtL systems can enhance liquid fuel yields and improve process economics, but it compromises environmental sustainability as the natural gas blending ratio increases. They concluded that the optimal natural gas blending ratio to meet the renewable fuel standard GHG emission targets from the U.S. environmental protection agency is up to 28%. Additionally, they highlight that achieving cost competitiveness with fossil-derived fuels requires optimizing blending ratios, heat integration, minimization of oxygen consumption, electricity, and excess hydrogen [27].

In terms of process conversion efficiency, GtL systems typically exhibit higher efficiency (~70%) depending on their reforming technology [9,27,28] compared to the BtL systems which is around half of this amount [7,27]. The GBtL process optimizes the syngas composition, overcoming the hydrogen deficiency of BtL syngas. This hybrid approach leads to higher efficiency compared to the BtL systems in the Fischer-Tropsch synthesis, providing an advantage over conventional BtL plants. See, for example, the figures about the carbon efficiency (Fig. 7 of the manuscript and Fig. S5 of the supplementary material).

Economically, GtL systems have traditionally been more favorable due to their higher efficiency and lower operational complexity and produced fuel costs [22]. However, the integration of biomass in GBtL systems allows for a significant reduction in greenhouse gas emissions, and particularly in the carbon footprint, due to less reliance on fossil fuel feedstock while maintaining cost-competitiveness with conventional GtL processes. The economic feasibility of BtL remains more challenging, largely due to lower process efficiency and higher capital costs. Still, BtL offers a distinct advantage in environmental sustainability, which is becoming increasingly valued in the current market landscape [26,27].

The inherent trade-offs between the economic and environmental criteria underscore the necessity for comprehensive assessments to determine the optimal conditions for GBtL systems, including identifying the most suitable feedstock ratio. Hence, a thorough examination of the operational conditions considering the utilization of various feedstock is still lacking and is essential to address the complex interplay of economic and environmental concerns. Compared to the previous works on GBtL process, this study includes biomass feedstock analysis, comprehensive environmental impact assessment using ReCiPe, and in-depth sensitivity analysis of operational parameters.

In this work, we contribute to this research direction to minimize the uncertainties surrounding the GBtL process by conducting a techno-economic and environmental assessment using several biomass feedstocks. We rely on a combination of process simulation tools (all unit operation performances are validated with experimental data) and detailed Life Cycle Assessment (LCA) methodologies to explore the implications of the integration, finding optimal process conditions and comparing various feedstock scenarios to establish a versatile integrated process that can adapt to challenges impacting the supply chain.

2. Methodology

2.1. Process description and simulation overview

The GBtL process was modeled in Aspen Plus v11 considering that feedstock can be varied between natural gas and different types of

biomass; however, the total input carbon of the system is kept fixed for comparison. Currently, there is no commercial hybrid GBtL plant, therefore laboratories and plant data [9,29,30] are used for each unit independently to validate the entire hybrid simulation model. The simulation result and validation of the integrated GBtL plant are provided in the Supplementary Material, Tables S1, S2 and S3. Post-processing of the simulation data is performed using 11 calculator blocks, which include more than 20 unit operations and 200 input variables. Around 100 output results of the model are subsequently used for sizing, calculating equipment cost and environmental impacts. The GBtL plant has four main subsystems (see Fig. 1(a)): feed preparation (grinding, drying and pre-reformer), syngas production (gasification and SMR), syngas treatment (CO_2 and water removal) and, FT and product upgrading. In addition, the BtL plant needs utilities such as steam, water, and oxygen. The required facilities for utilities and an air separation unit (ASU) for oxygen supply are included in the model (feed preparation subsystem). BtL and GtL plants have very similar process diagrams aside from the syngas production section. Fig. 1(b) illustrates a simplified block diagram of a GBtL process. The simulated flowsheet of the plant is shown in Fig. S1 of the Supplementary Material.

The capacity of the GBtL system is considered 17000 bbl/day according to the operating data of one train of the Oryx GtL plant in Qatar

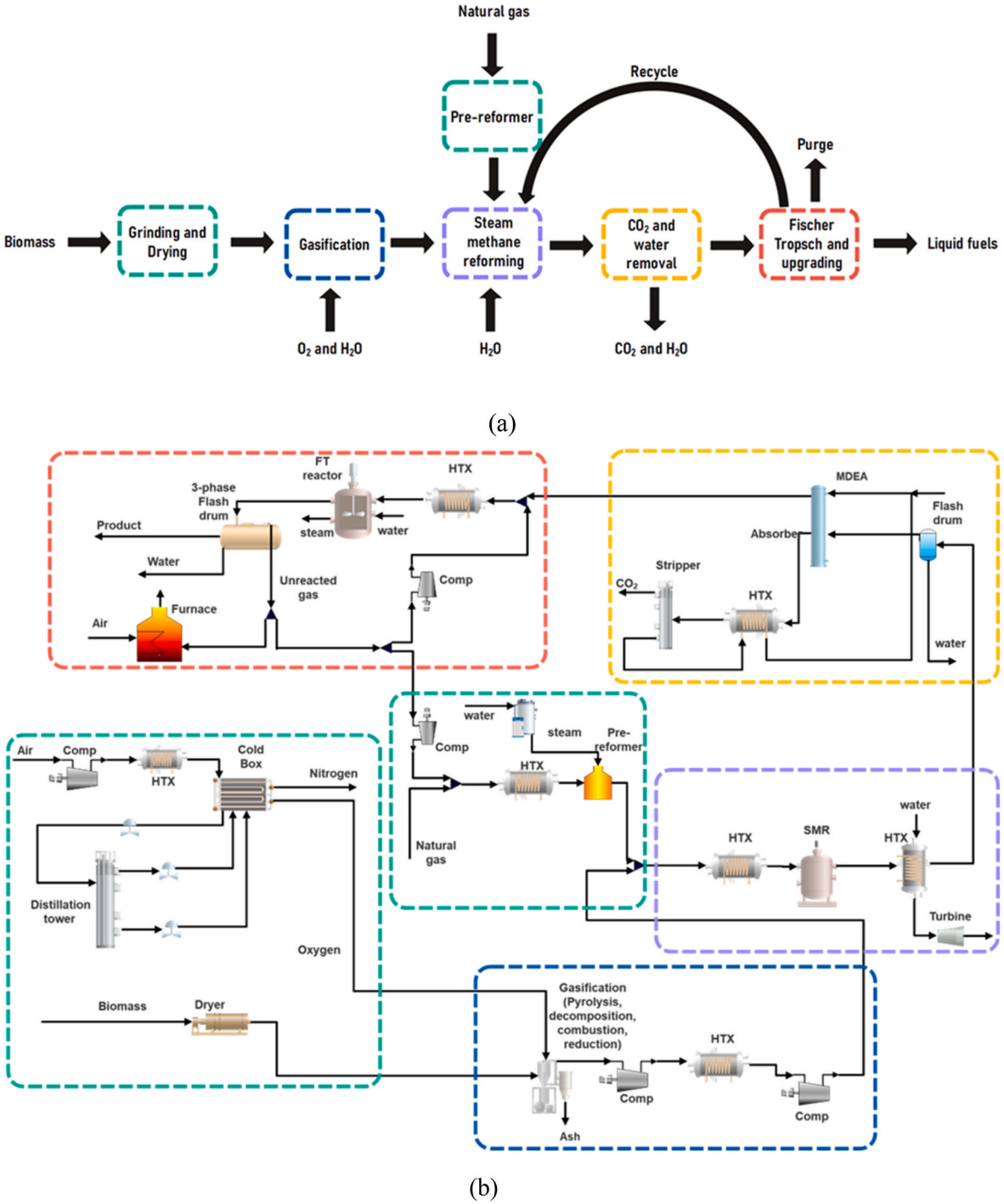

Fig. 1. Schematic of a typical GBtL process (HTX: heat exchanger, Comp: compressor; SMR: Steam methane reforming). a) Block diagram of the main subsystems of the GBtL process; b) Simplified flowsheet of the GBtL process (The heat integration is not considered in the figure).

[31]. The ratio of feedstock among biomass and natural gas (B:NG) is adjusted according to the economic and environmental objectives while the total mole flow of input carbon is constant. Based on available data and rough estimations, for producing 1 bbl of LFs, around 10 thousand standard cubic feet of natural gas is needed [28]. In the modeled GBtL plant, biomass feedstock passes through a gasification unit where steam and oxygen are injected to produce high-quality syngas. On the other hand, the SMR reactor is employed to produce hydrogen-rich syngas from natural gas feedstock. Notably, the syngas produced from gasification contains methane so it can pass through the SMR reactor. The final syngas contains significant amounts of H_2O and CO_2 which should be removed prior to the FT reactor to increase the efficiency and conversion rates. The FT product is divided into water, liquid hydrocarbons and unreacted gas fractions which are directed to a water treatment plant, upgrading section and recycle line, respectively. Part of the recycle stream is allocated for providing the required thermal energy demands of the plant while the remainder is recycled into FT and gasification units.

2.1.1. Feed preparation

There is a wide range of biomass types from wood chips to green or municipal wastes that can be utilized as feedstock. In this study, Pine pellet is considered as feedstock for the baseline scenario and the results are compared with other sources of biomass. Grinding and drying units handle biomass feedstocks to prepare them for gasification [22]. Biomass is defined as an unconventional component in Aspen Plus and it is modeled using UltAnal and ProxAnal (i.e., ultimate analysis and proximate analysis, respectively) as shown in Table 1. One of the main challenges to utilizing biomass on an industrial scale is the supply chain and the availability of a unique biomass feedstock throughout the entire year [32] so the final result of the baseline feedstock will be compared with other types of biomass.

As we use processed natural gas, there is no necessity for sweetening; however, since the natural gas line contains heavier hydrocarbon (propane, butane, etc.) a pre-reformer converts these materials to syngas and methane to increase the process efficiency. Natural gas contains 94.50% methane, 2.70% ethane, 1.48% propane and 0.80% nitrogen. The pre-reformer converts the ethane and propane in a stoichiometry reactor followed by an equilibrium reactor where the CO methanation and WGS reactions take place according to the operating conditions. The details of the reactions for the pre-reformer can be found in Table 2.

The total carbon flow rate as feedstock is kept fixed, and when the amount of biomass is specified, the amount of natural gas is calculated automatically.

2.1.2. Syngas production

Gasification is a thermochemical process that comprises pyrolysis, combustion and reduction zones. Among the currently developed technologies for gasification reactors, bubble-fluidized and entrained-flow reactors stand out for their high carbon conversion. Although the entrained-flow reactor provides better quality syngas, it consumes abundant oxidants and needs high temperature, so the average production cost of syngas is expected to be lower in the bubbling fluidized bed reactors [6,33,34]. In this study, we opted for the fluidized bed reactor to balance capital costs and syngas yield.

There are sets of complex reactions that occur in the gasification reactors. Some studies have tried to mimic this behavior with an equilibrium reactor or minimizing the Gibbs energy [35,36]. However, experimental data proved that except for narrow process conditions, the equilibrium reactions cannot predict the syngas produced in the overall range of operating conditions [37]. Thus, a reliable approach is to approximate the complex process by different sets of reactions for divided subprocesses.

Pyrolysis reactions are detailed in Table 2 where the reaction rate of each substance is defined as a function of temperature. The following assumptions are made for the gasification section: Reactor without pressure drop or temperature profile, one-dimension reaction section is considered and there is no change in the radial vector, ash is inert, and the decomposition zone converts all char and tar to the elemental species.

The pyrolysis reactions are modeled in a stoichiometry reactor, followed by a decomposition process that converts the char into its constituent components. In the next stage, oxygen is injected into the pyrolysis outlet gas for the combustion and reduction sections, which are approximated with two plug flow reactors in series, where 6 and 8 power-law reactions are taking place respectively (see Table 2 for more details).

The result of the gasification unit for different feedstocks is validated with experimental work [30]. Downstream units require high-pressure gas, so a compression section is needed. A boiler is utilized to generate saturated steam from the hot discharge of the compressors.

The quality of the syngas produced at the gasification reactor is improved by the use of agents, such as oxygen and steam [15,38]. Although air injection is price-wise and has been investigated in many studies [12,14] establishing an expensive ASU reduces the final expenses by taking into consideration that the presence of a large amount of nitrogen increases the size of all downstream units and lowers reaction efficiencies. The ASU has a good economy of scale, and it is utilized in gigantic plants such as the Pearl GtL plant with a capacity of 140,000 bbl/day production. A conventional cryogenic ASU [39] with an oxygen purity of more than 95% (molar) is simulated to supply the oxygen for the gasification unit. Nitrogen with a purity of over 99% (molar) is a value-added byproduct of the ASU plant. The compressed air passes through a heat exchanger, cold box and Joule–Thomson valve before entering the cryogenic distillation unit. The liquid oxygen and nitrogen gas from the distillation tower cross the cold box to cool the feed line before leaving the ASU.

An SMR does syngas production from natural gas feedstock to get the highest H_2/CO ratio [9]. SMR plays a critical role in the GBtL process by producing hydrogen-rich syngas with an H_2/CO ratio of 3–6. The endothermic nature of SMR requires precise temperature control, with methane reacting with steam to produce CO and hydrogen. Integrating SMR with biomass gasification enables the enrichment of the H_2 content in syngas, optimizing it for FT synthesis.

The SMR reactions are simulated in a plug flow reactor with 3 Langmuir Hinshelwood Hougen Watson (LHHW) kinetics (Table 2) which operates at 1100 K [40]. The simulated reactor is validated with experimental data [29], and the catalyst loading in the SMR is tuned to

Table 1
Biomass feedstock elemental analysis for the different feedstocks considered [30].

Biomass	Proximate analysis (wt %) wet basis				Ultimate analysis (wt %)				
	Moisture	Fixed carbon	Volatile matter	Ash	C	H	N	S	O
Pine Pellet (baseline)	4.60	16.60	78.50	0.30	47.50	6.20	0.09	0	46.21
Wood pellet	6.30	11.20	82.00	0.50	47.76	5.95	0	0	46.29
Eucalyptus A	11.80	14.60	71.00	2.87	45.85	6.13	0.35	0	47.67
Eucalyptus B	11.40	19.00	68.50	1.19	49.07	6.45	0.07	0	44.41

Table 2
Reactions and kinetic rates.

Pre-reformer [9]	
$C_nH_{2n+2} + nH_2O \rightarrow nCO + (2n+1)H_2$	Conversion = 100% (n = 2, 3)
$C_nH_{2n} + nH_2O \rightarrow nCO + (2n)H_2$	Conversion = 100% (n = 2, 3)
SMR [40]	
$CH_4 + H_2O \leftrightarrows CO + 3H_2$	$r_1 = k_1 \frac{\left(\frac{P_{CH_4}P_{H_2O}}{P_{H_2}^{2.5}} - \frac{P_{CO}P_{H_2}^{0.5}}{K_{eq_1}}\right)}{DEN^2}$
$CH_4 + 2H_2O \leftrightarrows CO_2 + 4H_2$	$r_2 = k_2 \frac{\left(\frac{P_{CH_4}P_{H_2O}^2}{P_{H_2}^{3.5}} - \frac{P_{CO_2}P_{H_2}^{0.5}}{K_{eq_2}}\right)}{DEN^2}$
$CO + H_2O \leftrightarrows CO_2 + H_2$	$r_3 = k_3 \frac{\left(\frac{P_{CO}P_{H_2O}}{P_{H_2}} - \frac{P_{CO_2}}{K_{eq_3}}\right)}{DEN^2}$
$DEN = 1 + K_{CH_4}P_{CH_4} + K_{H_2}P_{H_2} + K_{CO}P_{CO} + K_{H_2O}P_{H_2O}/P_{H_2}$	
$K_{eq_1} = \exp\left(\frac{-26830}{T} + 30.114\right)$	$k_1 = 1.17 \times 10^{15} \times \exp\left(\frac{-240100}{RT}\right)$
$K_{eq_2} = K_{eq_1} \times K_{eq_3}$	$k_2 = 2.83 \times 10^{14} \times \exp\left(\frac{-243900}{RT}\right)$
$K_{eq_3} = \exp\left(\frac{4400}{T} - 4.036\right)$	$k_3 = 5.43 \times 10^5 \times \exp\left(\frac{-67130}{RT}\right)$
$K_{CH_4} = 6.65 \times 10^{-4} \times \exp\left(\frac{38280}{RT}\right)$	$K_{CO} = 8.23 \times 10^{-5} \times \exp\left(\frac{70650}{RT}\right)$
$K_{H_2} = 6.12 \times 10^{-9} \times \exp\left(\frac{82900}{RT}\right)$	$K_{H_2O} = 1.17 \times 10^5 \times \exp\left(\frac{-88680}{RT}\right)$
Pyrolysis [46]	
$Y_{H_2} = 1.362 \times 10^{-5} T^2 - 0.02517\, T + 12.19$	$Y_{CO} = -3.524 \times 10^{-5} T^2 + 0.0977\, T - 24.93$
$Y_{CO_2} = 3.958 \times 10^{-5} T^2 - 0.09126\, T + 64.02$	$Y_{CH_4} = -4.341 \times 10^{-5} T^2 + 0.1012\, T - 51.08$
$Y_{H_2O} = 5.157 \times 10^{-5} T^2 - 0.1186\, T + 84.91$	$Y_{C_2H_4} = -6.873 \times 10^{-5} T^2 + 0.1494\, T - 76.89$
$Y_{C_2H_6} = 8.265 \times 10^{-6} T^2 - 0.02105\, T + 13.38$	$Y_{C_6H_6} = -3.134 \times 10^{-5} T^2 + 0.07544\, T - 42.72$
$Y_{C_2H_6O} = 1.508 \times 10^{-5} T^2 - 0.03662\, T + 22.19$	$Y_{C_7H_8} = -4.539 \times 10^{-6} T^2 + 0.00687\, T + 1.462$
$Y_{C_{10}H_8} = -8.548 \times 10^{-6} T^2 + 0.01882\, T - 9.851$	
Combustion zone [30]	
$1.25C + O_2 \rightarrow 0.5CO + 0.75CO_2$	$r = 3.7 \times 10^{10} T \times \exp\left(\frac{-150000}{RT}\right)[O_2]$
$CO + 0.5O_2 \rightarrow CO_2$	$r = 1.78 \times 10^{10} \exp\left(\frac{-180000}{RT}\right)[CO][O_2]^{0.25}[H_2O]^{0.5}$
$CH_4 + 0.5O_2 \rightarrow CO + 2H_2$	$r = 1.58 \times 10^{12} \times \exp\left(\frac{-202000}{RT}\right)[O_2]^{0.8}[CH_4]^{0.7}$
$H_2 + 0.5O_2 \rightarrow H_2O$	$r = 1.08 \times 10^7 \times \exp\left(\frac{-10800}{RT}\right)[O_2][H_2]$
$C_6H_6O + 4O_2 \rightarrow 6CO + 3H_2O$	$r = 655 \times \exp\left(\frac{-80200}{RT}\right)[O_2][C_6H_6O]^{0.5}$
$C_6H_6 + 4.5O_2 \rightarrow 6CO + 3H_2O$	$r = 2.4 \times 10^{11} \exp \times \left(\frac{-126000}{RT}\right)[O_2][C_6H_6]^{0.5}$
Reduction zone [30]	
$C + H_2O \rightarrow CO + H_2$	$r = 0.008 \times \exp\left(\frac{-49900}{RT}\right)[C][H_2O]$
$CO + H_2O \rightarrow CO_2 + H_2$	$r = 278 \times \exp\left(\frac{-12600}{RT}\right)[CO][H_2O]$
$CO_2 + H_2 \rightarrow CO + H_2O$	$r = 258 \times \exp\left(\frac{-12600}{RT}\right)[CO_2][H_2]$
$CH_4 + H_2O \rightarrow CO + 3H_2$	$r = 4.92 \times 10^{-11} \exp\left(\frac{-125000}{RT}\right)[H_2O][CH_4]$
$C + CO_2 \rightarrow 2CO$	$r = 1.05 \times 10^{13} \times \exp\left(\frac{-135000}{RT}\right)[C]$
$C_6H_6O \rightarrow CO + 0.4C_{10}H_8 + 0.15C_6H_6 + 0.1CH_4 + 0.75H_2$	$r = 10^7 \times \exp\left(\frac{-100000}{RT}\right)[C_6H_6O]$
$C_6H_6O + 3H_2O \rightarrow 4CO + 0.5C_2H_4 + CH_4 + 3H_2$	$r = 10^7 \times \exp\left(\frac{-100000}{RT}\right)[C_6H_6O]$

Table 2 (*continued*)

Pre-reformer [9]	
$C_{10}H_8 \rightarrow 6.5C + 0.5C_6H_6 + 0.5CH_4 + 1.5H_2$	$r = 1.7 \times 10^7 \times \exp\left(\frac{-350000}{RT}\right)\frac{[C_{10}H_8]^{1.6}}{[H_2]^{0.5}}$
WGS reactor	
$CO + H_2O \leftrightarrows CO_2 + H_2$	$K_{eq} = \exp\left(\frac{4577.8}{T} - 4.33\right)$
FT reactor [9]	
$nCO + 2nH_2 \rightarrow (-CH_2-)_n + nH_2O + \Delta H\ (>0)$ (n = 1 − 20 and n = 25 for wax cut)	$r_{CH_4} = \frac{3.667 \times 10^{-9} P_{H_2} P_{CO}^{0.05}}{1 + (3.3 \times 10^{-5}) P_{CO}}$ $r_{CO} = \frac{6.655 \times 10^{-9} P_{H_2}^{0.6} P_{CO}^{0.65}}{1 + (3.3 \times 10^{-5}) P_{CO}}$

obtain high conversion (~90%); however, this conversion rate is reduced if the feedstock composition changes, as the steam feed flowrate in the SMR is affected [29]. As long as the produced syngas from biomass contains a high amount of methane, a route to convert it to syngas in the SMR reactor is considered. The injected steam into the SMR reactor is a parameter that allows modifying the H_2/CO ratio of the mixed syngas. According to the SMR kinetics outlined in Tables 2 and it is observed that the quantity of steam increases in scenarios characterized by lower hydrogen content, and conversely decreases when hydrogen content in the gasification is higher.

2.1.3. Gas treating

In this phase, the produced syngas is prepared for the FT synthesis. To do so, the mole fraction of CO_2 should be decreased to obtain a higher syngas conversion rate with the higher partial pressure of the reactants. A methyl diethanolamine (MDEA) CO_2 capture process with an absorber and a stripper is simulated using the ELENRTL thermodynamic package. The CO_2 to MDEA ratio is around 45% and the MDEA concentration in the solvent is near 35% w/w [41]. The heat integration of the plant provides the energy requirements to absorb more than 90% of the CO_2. The captured CO_2 can be stored or utilized in similar processes, such as WGS unit and urea production [42,43]. Conversion of CO_2 rich syngas to LFs can occur in the FT reactor but it requires the use of specific iron-based catalysts [44,45].

Removing the steam content of the produced syngas will increase the conversion rates of the FT reactor. A considerable amount of water content in the syngas is separated in a flash drum by lowering the syngas temperature. Then, the inlet stream of the FT reactor needs to be reheated to 210 °C [28].

2.1.4. Fischer-Tropsch reactor

In this section, the treated gas is passed through the FT slurry bubble column reactor (SBCR) and the unreacted gases are separated. The low-temperature FT (LTFT) reactors use Cobalt catalysts to provide a high production rate of wax. Cobalt catalysts are preferred for FT synthesis due to their higher selectivity for long-chain hydrocarbons at low temperatures. Iron catalysts are also employed in FT reactors, particularly at higher temperatures, for their effectiveness on WGS reaction [47]. We simulate the process using a slurry bubble column reactor, which provides efficient heat removal and appropriate catalyst distribution [28].

More than 40 LHHW kinetic reactions are involved in the formation of different olefins and paraffins [28]. The FT reactor generates a high amount of heat during its operation. To maintain an isothermal operating condition at 210 °C, pressurized steam is used as a coolant. Medium-pressure steam is generated from the released heat from the FT reactor. As a good approximation, the FT reactions in the SBCR are simulated in a continuous stirred-tank reactor (CSTR) with a volume of 2000 m^3. The catalyst volume fraction in the reactor is 10% with 2000 kg/m^2 density. To calculate the FT conversions, it is assumed that the weight fraction of Cobalt in the catalyst is 20% while the exposed surface atom of cobalt is 10% [28]. The details of the simulation of the FT

reactions with variable chain growth probability, where FT product distributions are a function of mole fractions of H_2 and CO in the FT reactor, are available in section 1 of the supplementary material.

Water and unreacted gas released from the FT reactor are separated from products in a 3-phase drum. A part of unreacted gas and light ends (tail gas) is recycled to the FT reactor to enhance the overall conversion of the reactor. As the GBtL process requires steam and heat, a part of tail gas, which is purged from the recycle loop is burnt in a furnace to supply the energy required.

2.2. Economic assessment

The total investment cost of the GBtL plant is estimated based on the Lang equation (eq. (1)) for most of the equipment and Peters et al. [48] study. It is assumed that the working capital cost is 15% of fixed capital cost and there are 330 working days per year. The NPV of the plant is evaluated using Equation (2). The detailed calculation and financial coefficients are available in Tables S4 and S5 of the supplementary materials.

$$\text{Equipment cost} = \text{Reference cost} \times \left(\frac{\text{Equipment capacity}}{\text{Reference capacity}}\right)^{\text{Factor}} \times \frac{\text{Cost index (2022)}}{\text{Reference cost index}} \quad \text{(eq. 1)}$$

$$\text{NPV} = \sum_{t=1\ to\ 25} \frac{\text{Cash flow}_t}{(1+\text{interest rate})^t} - \text{FCI} \quad \text{(eq. 2)}$$

2.3. Life cycle assessment

The environmental evaluation is carried out by LCA (a methodology for evaluating the environmental impacts associated with the entire life of the process) [49]. This study covers from cradle to gate, thereby involving all the activities before the usage phase of the LF. The LCA data is extracted from Ecoinvent by SimaPro software (background system) and the inventory data is collected from the simulation (foreground system). Environmental implications are assessed with the ReCiPe method [50]. The normalization and weighting factors facilitate comparing the environmental impact of the processes by indicating one score for each case [50]. The functional unit for environmental calculation is 1 barrel of LF.

In order to have a detailed environmental assessment of the process, it is imperative to define all plant inputs and outputs. The allocation in this study is selected in reference to a point of substitution (APOS) of Ecoinvent v.3.7 life cycle inventories. Global inventories are considered for most of the inputs and outputs. The produced nitrogen and electricity are assumed as by-products of the plant, and economic allocation is implemented to assess the final impact of the main product. To evaluate the equipment impact, it is assumed that they were constructed using steel although results express that the impact of equipment is negligible compared to other inputs. Also, 100-km transportation for the fuels is deemed.

2.4. Scenario development

Investigated scenarios involving the utilization of four types of feedstocks, as delineated in Table 1, considering their implications on both environmental and economic aspects.

Finding the optimal values for the free variables of the baseline plant is the case study. To do so, a sensitivity analysis is performed; Our analysis includes altering biomass feedstock from 150 to 200 tons/h (optimum range) and altering oxygen flowrate from 35 to 43 tons/h (valid range) for the baseline feedstock.

3. Results and discussion

The simulation outcomes including the main input and output data and the economic results can be found in the Supporting Information (Sections S1 to S3).

3.1. Different feedstock usage

The utilization of various feedstock (Table 3) throughout a year is assessed to find out the relation between the feedstock composition and the techno-economic condition of the integrated process of the GBtL plant. The profit is calculated by deducing the total production cost from the revenues. In this comparison, the carbon efficiency of the integrated plant is also considered as one of the main indicators. Carbon efficiency is defined as the total moles of carbon in the products divided by the total moles of carbon of input (feed and fuel).

Selection of the best feedstock always depends on various conditions such as supply chain, price, the efficiency of the process, etc. The results in Table 3 consider the same condition for supply chain and price. The Eucalyptus B feedstock has the highest profit and the best NPV while the wood pellet shows lower investment cost for the integrated plant.

Biomass supply will encounter several logistical and operational challenges. One of the primary issues is the geographical and seasonal variability in biomass availability. Since biomass is often harvested seasonally, supply fluctuations can cause price volatility and necessitate consideration of alternative feedstocks. Storage is another significant challenge, as biomass requires considerable space and has lower energy density compared to conventional fossil fuels. This often requires larger storage areas and increases the plant's costs. Additionally, transporting biomass over long distances poses economic and environmental issues, making it crucial for the plant to be located near biomass resources.By comparing Tables 1 and 3, it can be inferred that the amount of carbon content in the feedstock has a significant impact on the economics of the integrated plant, and as expected, the model is very sensitive to the carbon content of biomass. The seemingly small variation in carbon content in the Ultimate analysis between Eucalyptus B and pine pellets (less than 2%), plays a pivotal role in syngas production during gasification. This difference in carbon utilization efficiency between feedstocks affects the syngas production and downstream units, as higher carbon content in Eucalyptus B results in more CO generation and a larger volume of adjusted syngas, indirectly enhancing the SMR efficiency and economical of the entire process.

The hydrogen content, along with other substances such as oxygen, exerts an influence on the syngas quality; however, their impacts are generally mitigated by the introduction of steam and oxygen in the gasification unit. The high content of carbon in Eucalyptus B biomass results in higher production of CO during the gasification, which yields a greater amount of adjusted syngas (after SMR) destined for the FT reactor. Therefore, the higher conversion rate of both feedstocks into syngas is a critical bottleneck with the potential to enhance the overall economic viability of the GBtL system. The plant with the pine pellet biomass has the best efficiency regarding the usage of carbon content in feedstock, however, the LCA analysis can illustrate more detailed aspects.

Comparative analysis of the findings with those of prior studies [21,24,25] reveals that results are aligned by estimating the same proportional conditions. The high conversion rate of syngas in the FT reactor,

Table 3
Techno-economic comparison using various biomass feedstock.

Feedstocks	Profit [M$/year]	FCI [M$]	NPV [M$]	Carbon efficiency
Wood pellet	53.1	668	80.4	47.0%
Pine pellet	52.6	670	71.3	47.1%
Eucalyptus A	−13.6	752	−943.6	44.0%
Eucalyptus B	61.8	692	179.0	46.7%

optimal condition of the feedstock, implementation of the heat integration and incorporation of recycle streams result in relatively more favorable economic conditions and consequent reduction in the TPC of the integrated GBtL plant.

Various biomass feedstock demonstrates the different intensity of impacts for each ReCiPe category (Fig. 2). As expected, there is no alternative that performs best in all (or most) impact categories. Selecting the optimum biomass ratio in the feed is mainly dependent on the supply chain and location of the plant. For example, although the wood and pine pellet feedstocks show less global warming impacts, they occupy more land and consume more water and those aspects should be carefully considered, in addition to the local characteristics of each region [51]. Thus, stakeholders can use Fig. 2 to select the appropriate biomass in accordance with their particular criteria. The distribution of environmental impacts demonstrates that most of the impacts derive from processing, where the produced syngas from biomass consumes a high amount of electricity in compressors. However, future decarbonization of the electricity grid is expected to significantly diminish these electricity-related impacts [52].

The endpoint ReCiPe approach can condense the number of indicators from 18 to three main categories (Human health, ecosystems and resources). The standard weighing factors of the ReCiPe method [50] are employed to yield a single score for each type of feedstock. The calculated scores for pine pellet, eucalyptus A, eucalyptus B and wood pellet are 4.91, 7.16, 6.77 and 4.34, respectively. From a general perspective, the wood pellet and pine pellet biomass attain better environmental performances, as evidenced by their achievement of lower scores.

3.2. Sensitivity results

In this section, we delve into the influence of the blending ratio of biomass and natural gas and the oxygen flow rate on the economic and environmental results for the baseline feedstock. The pine pellet has been chosen as the designated biomass feedstock for all the subsequent analyses and evaluations. As explained, the blending ratio of feedstocks (B:NG) is designed as a free variable. To calculate the optimum blending ratio, a sensitivity analysis that manipulates the biomass mass flow rate from 150 tons/h to 200 tons/h (optimum range) is performed; natural gas, oxygen and steam are adjusted automatically based upon a fixed amount of carbon input and optimum syngas production, so all cases are comparable as shown in Fig. 3 for the baseline feedstock. The sensitivity of the plant's profitability to changes in feedstock and product prices is shown in Fig. S5 of the supplementary material, which highlights the strong effects of biomass and wax prices on the plant's economy.

The profit of the plant has an optimum point where the biomass-to-natural gas mass ratio is around 4.27. The optimal blending ratios for the other feedstocks are calculated in a similar approach in Fig. S4 and Table S6 of the supplementary materials. Total production cost (TPC) and revenue affect the economic indicators. TPC includes a variety of fixed and variable expenses such as raw materials, operating labor, depreciation, and maintenance … [48], while the revenue is derived from selling the different hydrocarbon products (gasoline, kerosene, etc.) in addition to the nitrogen obtained in the ASU as a byproduct. The raw material costs (feedstocks) have the largest share in the TPC of the GBtL plant which directly affects the profit (detailed information is available in Fig. S3 of the supplementary materials).

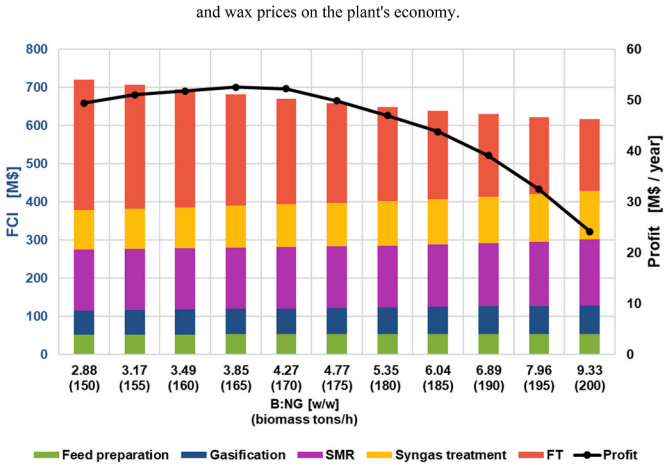

Fig. 3. Effect of the feedstocks blending ratio (biomass: natural gas) on the process economics for the pine pellet biomass.

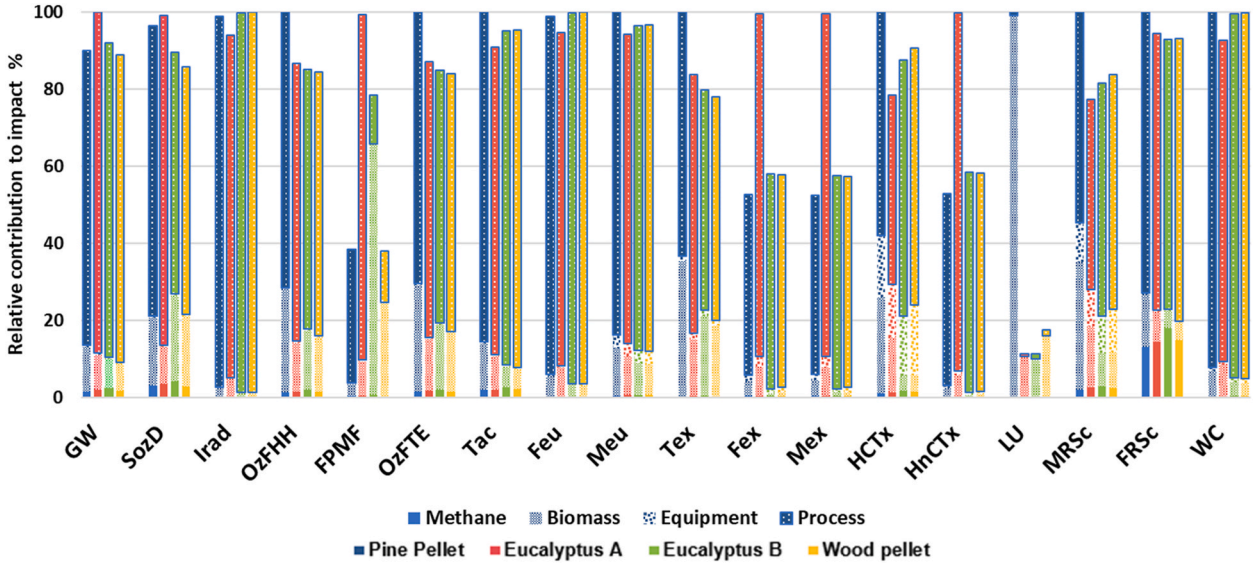

Fig. 2. Comparison of environmental impacts of various biomass feedstock. GW: Global warming; SozD: Stratospheric ozone Depletion; Irad: Ionising radiation; OzFHH: Ozone Formation, Human Health; FPMF: Fine Particulate Matter Formation; OzFTE: Ozone Formation, Terrestrial Ecosystems; Tac: Terrestrial acidification; Feu: Freshwater eutrophication; Meu: Marine eutrophication; TEx: Terrestrial Ecotoxicity; Fex: Freshwater ecotoxicity; Mex: Marine ecotoxicity; HCTx: Human Carcinogenic Toxicity; HnCTx: Human non-Carcinogenic Toxicity; LU: Land Use; MRSc: Mineral Resource Scarcity; FRSc: Fossil Resource Scarcity; WC: Water Consumption.

As the total carbon input from the feedstock is fixed and the hydrogen-to-carbon monoxide ratio is adjusted by changing the manipulated variables (i.e., steam and oxygen), the production rate remains relatively stable [9], even with changes in the feedstock ratio. This is because the syngas produced from both feedstocks is carefully controlled using calculator blocks and design specifications in the simulation, ensuring minimal variation in the distribution of hydrocarbons in the FT reactor across the operating range. However, note that FT products distribution is a function of chain growth probability (α), which is a function of H_2/CO, and this is incorporated in our detailed FT reactor [9]. Although a slight uptick in production is observed due to the increasing nitrogen byproduct in the ASU, the revenue from FT products exhibits a flat maximum at around 170 tons/h of biomass consumption due to higher production, as shown in Fig. 3 (see Table S5 of the supplementary materials).

TPC is linked to three main categories, which vary independently: utility cost, fixed capital investment (FCI) and raw materials (check Fig. S3 and Table S4 of the supplementary material for the TPC distribution). Utility cost is one of the key parameters to shape Fig. 3 decline trend because by expanding the biomass share in feedstock, the electricity sharply increases due to the compressors and refrigerant consumption in the ASU. This means that the BtL process (or high B:NG) does not present a favorable return on investment in comparison with GtL (or low B:NG). On the other hand, the raw materials cost has a positive effect by increasing the sharing part of the biomass on the economy of the plant. Generally, the total production cost of biofuel (a part of the LFs produced from biomass conversion) is more expensive than that of fossil fuel (a part of the LFs produced from methane conversion) due to the high oxygen and electricity consumption during the BtL process.

The FCI linearly diminishes by increasing the biomass blending ratio (Fig. 3), indicating that the integrated GBtL plant has a higher FCI compared to a standalone BtL plant [25]. The costs of equipment such as compressors and heat exchangers grow by increasing the biomass feedstock, while the cost of other unit operations such as the furnace decrease due to lower recycle flowrate. The main contribution to the reduction of the FCI is correlated to the reactors (more than 50% of the FCI, check Fig. S2 of the supplementary material for the details). Catalyst expenses make up approximately 20% of the total cost for each catalytic reactor, which is consistent with economic calculations, making their cost a critical factor in the economic assessment. The FT reactor and its catalyst form the most significant cost component, followed by the SMR unit. The syngas treatment, gasification, and feedstock preparation units contribute to the FCI to a lesser extent.

The feed preparation, gasification and syngas treatment units require more investment by increasing the share of biomass, while the FT reactor cost significantly drops because of the substantial reduction of the recycle flow rate by increasing the B:NG ratio. This flow reduction is primarily attributed to the amount of injected steam in the SMR unit, which adjusts the H_2/CO ratio in the synthesis gas. By expanding the biomass share in the feedstock, the required steam for the SMR is increased, which subsequently affects the SMR efficiency and the recycle flow rate. The cost of the SMR reactor has minor oscillations because the amount of natural gas and recycle flowrate diminish while the amount of syngas produced in the gasification unit rises.

The oxygen flowrate in the gasification unit is another crucial free variable for the quality of syngas, so in Fig. 4 we analyze this effect on the profit of the integrated plant.

The amount of syngas production from the gasification unit can explain the rationale behind the oscillating trend of the plant profit in Fig. 4. Kinetics of the gasification (Table 2) demonstrates a local minimum for syngas production at 41 tons/h of oxygen. A wider range of oxygen mass flow leads to the violation of the valid operating temperature of the gasification unit. Therefore, the flow rates are analyzed between 35,000 and 43,000 kg/h to maintain the gasification temperature between 700 and 1000 °C, [6,37]. The higher temperature range

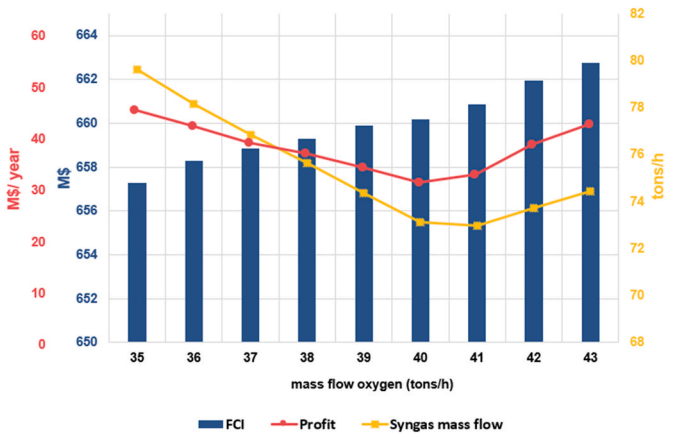

Fig. 4. Effect of the oxygen flowrate on the process economics for the pine pellet biomass.

provides more H_2 and a better quality of syngas; however, it also increases ash-related problems, such as agglomeration [37]. Conversely, lower temperatures result in increased tar content, which creates operational problems in downstream units. The higher production of syngas improves the whole process efficiency and reduces the amount of the recycle flow rate. The FCI demonstrates a consistent upward trend due to the expansion of ASU by increasing the oxygen flow rate.

The economics of an integrated process without the recycle stream is also studied and compared with the base case. The excess amount of energy in the furnace is employed to generate steam and electricity for the simulation scenario without the recycle stream. Eliminating the recycling stream reduces production by more than 15% of the production which leads to a change of just nearly 100 million dollars per year in profit (10% of the profit). Nonetheless, the amount of FCI diminished by around 150 million dollars (20%) because of the elimination of two compressors and the smaller size of some equipment.

Fig. 5 illustrates that increasing the B:NG has negative consequences from environmental aspects because the BtL process is more complex and less efficient compared to the GtL process. Thus, enlarging the biomass share in feedstock leads to higher consumption of utilities and resources. Eliminating the recycling stream decreases the availability of the purge stream as fuel, and therefore the environmental impacts increase by around 10% in this scenario. The distribution of impacts is

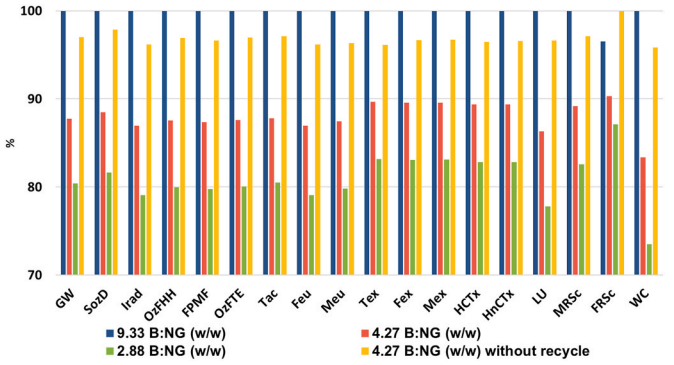

Fig. 5. Distributed environmental impacts comparing different blending ratios of the baseline feedstock. GW: Global warming; SozD: Stratospheric ozone Depletion; Irad: Ionising radiation; OzFHH: Ozone Formation, Human Health; FPMF: Fine Particulate Matter Formation; OzFTE: Ozone Formation, Terrestrial Ecosystems; Tac: Terrestrial acidification; Feu: Freshwater eutrophication; Meu: Marine eutrophication; TEx: Terrestrial Ecotoxicity; Fex: Freshwater ecotoxicity; Mex: Marine ecotoxicity; HCTx: Human Carcinogenic Toxicity; HnCTx: Human non-Carcinogenic Toxicity; LU: Land Use; MRSc: Mineral Resource Scarcity; FRSc: Fossil Resource Scarcity; WC: Water Consumption.

almost the same as in Fig. 2, where the produced syngas from biomass and the electricity consumption of the compressors are the most significant. Therefore, changing the B:NG does not affect each impact category in a different way so the best and worst scenario remains the same for all the categories.

3.3. Biogenic carbon

We performed a cradle-to-gate LCA, thus the consumption stage of fuels is not included. However, one of the main reasons for using biomass as renewable feedstock is the contribution of biogenic carbon sources to LCA, and therefore the absorbed carbon in the biomass will come back into the environment by combustion of fuel (cradle-to-wheel LCA). Including this aspect clearly highlights the use of biomass as a renewable feedstock [53,54]. Fig. 6 explains how this aspect affects the ranking of the different scenarios considered in the environmental analysis.

Fig. 6 expresses that going toward biomass feedstock diminishes the released carbon dioxide by the negative impact of biogenic carbon [55]. The combustion emissions have negligible differences for the scenarios as the quality of the produced LF is similar and the variation is due to the difference in the production capacity. For the scenario with the lowest amount of biomass, the total CO_2 equivalent emission reaches nearly 200 kg per barrel while for the scenario with the highest percentage of biomass, it is around 130 kg per barrel. Thus, increasing the amount of biomass in feedstock from 150 tons/h to 200 tons/h could reduce the total global warming impacts by over 30%.

The primary influential factor concerning the global warming indicator of the GBtL plant pertains to carbon efficiency and the effective utilization of the feedstock carbon. The integration of the GtL and the BtL plants aims to enhance this synergic effect. Fig. 7 demonstrates how the input carbon is exploited in the GBtL plant (check the supplementary file Fig. S6 for the BtL and GtL carbon routes). The carbon efficiencies are approximately 23%, 50% and 70% for the BtL, GBtL and GtL plants, respectively (check Section 3 in the supplementary materials). By increasing the share of natural gas in the GBtL process, not only the carbon efficiency of the overall plant will sharply grow, but also the

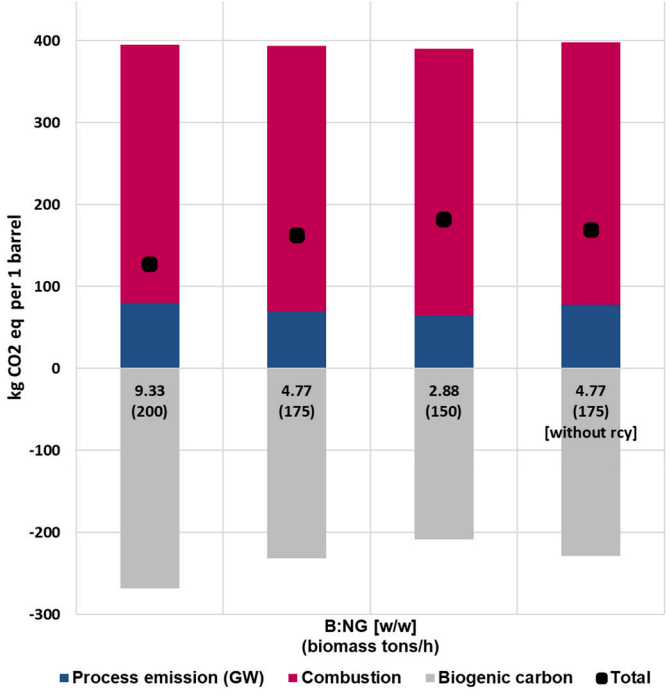

Fig. 6. Global warming impacts of the baseline scenario comparing different feedstock blending ratios.

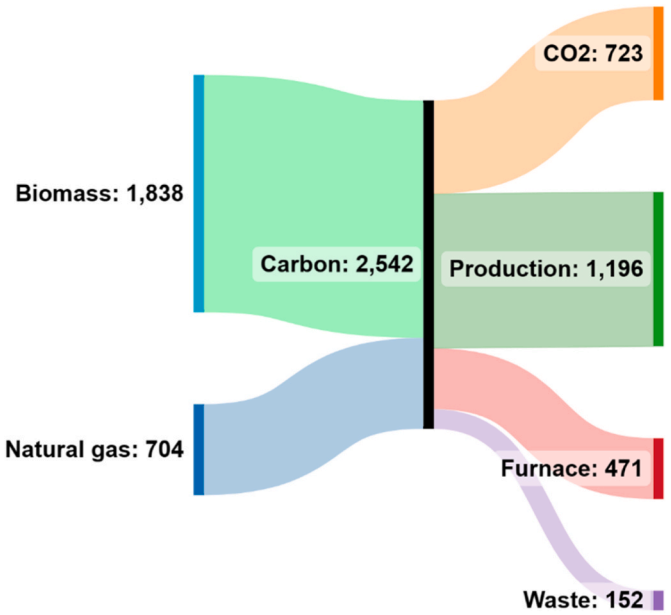

Fig. 7. Carbon route in tons per day for the GBtL process.

carbon recovery of the biogenic carbon (biomass) will experience a significant enhancement. It is worth mentioning that approximately similar efficiencies are mentioned in the literature; however, these percentages are highly influenced by operational conditions [27,28,56] and the technology selected. The 70% GtL carbon efficiency was achieved by employing auto-thermal reformers for syngas production, and 50% of the GBtL efficiency was obtained after the optimization (see the sensitivity results section). It is assumed that the BtL process has only one recycle loop around the FT reactor and a part of the feedstock is used for heat generation for all the plants.

Around 72% of carbon (865 tons per day) of the final product is supplied by the bio-genic source in the suggested GBtL plant which is more than 75% (372 tons of carbon) increase compared to the stand-alone BtL plant (check the Supplementary Material Fig. S6 for the BtL carbon route). Therefore, the recovery of biogenic source of carbon (biomass) into the final product can be significantly enhanced (approximately 20%) by integrating biomass plants with fossil fuel resources.

4. Conclusions

The utilization of various sources of biomass influences economic metrics in different aspects. The amount of carbon and ash in the analyzed biomass types are crucial parameters for the economic performance and environmental impact of the plant. Higher carbon content in the biomass boosts the profit while low hydrogen content enhances the SMR conversion and consequently carbon efficiency of the integrated process increases. Thus, the comparison between the usage of four different feedstocks demonstrates that the selection of Eucalyptus B, with higher hydrogen and carbon content, is more profitable. The feedstock selection affects the process conditions and utility requirements which plays a significant role in the environmental impacts. For instance, the single environmental score (normalized impact) for the wood pellet is approximately twice that of the Eucalyptus B feedstock. Due to the difficulties in continuously supplying a unique type of biomass all over the year for industrial plants, a detailed comparison of mixed biomass feedstocks should be considered; the final decision for the optimal feedstock selection should be based on regional conditions and policies.

A sensitivity analysis is conducted to study the optimal process conditions of the baseline GBtL plant. The economy of the integrated

plant is evaluated based on profit and NPV. The optimum economic result is achieved when the biomass mass weight is 4.27 times higher than natural gas which results in the daily production of above 13500 barrels of liquid fuels. This level of production is 20% lower compared to an existing GtL facility and around 50% higher compared to a BtL plant, assuming equivalent carbon input in the feedstock. Changing the B:NG does not considerably affect the production capacity due to operating variables operating in the optimum region, so the optimum ratio for the integrated plant is due to a trade-off between the utility costs, the FCI and the efficiency of the syngas production unit.

The recycle flow rate varies in each case and has a significant impact on economics due to its effect on the blending ratio. A higher percentage of biomass in the feedstock leads to producing insufficient H_2 in the gasification, which is compensated by a higher steam rate in the SMR. Consequently, the overall efficiency of the syngas production is enhanced with a higher utility cost and it decreases the recycling stream. This result indicates that for a high B:NG, the reduction (or even elimination) of the recycle line is preferable.

The high electricity consumption is the main contribution to the environmental analysis, although future decarbonization of the electricity mix will decrease the impacts. Expanding the share of biomass feedstock leads to increased compressor loads; consequently, the overall environmental impact will be worse in most of the ReCiPe categories. However, considering the final step of the life cycle of carbon (usage phase of the LFs) shows an opposite inference due to the release of biogenic carbon dioxide from the biomass feedstock. Thus, increasing the biomass (i.e., biogenic carbon) by 50 tons/h (33%) can reduce the global warming impact of the integrated process by 30%, while the total amount of carbon in the feedstock is fixed.

Nomenclature

ASU	Air Separation Unit
B:NG	Biomass to natural gas ratio
BtL	Biomass to liquid
CSTR	Continuous stirred-tank reactor
CtL	Coal to liquid
CBtL	Coal and biomass to liquid
GBtL	Natural gas and biomass to liquid
GHG	Greenhouse gas
GtL	Natural gas to liquid
FCI	Fixed capital investment
FT	Fischer-tropsch
h	hour
HTX	Heat exchanger
R	Gas constant [J/K·mol]
LCA	Life cycle assessment
LFs	Liquid fuels
LHHW	Langmuir Hinshelwood Hougen Watson
MDEA	Methyl diethanolamine
P	Partial pressure [N/m^2]
PtL	Power to liquid
SMR	Steam methane reforming
T	Temperature [K]
TPC	Total production cost
WGS	Water gas shift

CRediT authorship contribution statement

Mostafa Zarandi: Writing – original draft, Visualization, Validation, Software, Methodology, Investigation, Formal analysis. **Mehdi Panahi:** Writing – review & editing, Data curation, Conceptualization. **Ahmad Rafiee:** Investigation, Conceptualization. **Sajad Namazi Rad:** Validation, Formal analysis, Data curation. **Ángel Galán-Martín:** Writing – review & editing, Supervision. **Josep M. Mateo-Sanz:** Supervision, Resources, Funding acquisition. **Laureano Jiménez:** Writing – review & editing, Supervision, Resources, Project administration, Funding acquisition.

Declaration of generative AI and AI-assisted technologies in the writing process

During the preparation of this work the authors used openAI's chatGPT in order to improve language and readability, with caution. After using this tool/service, the authors reviewed and edited the content as needed and take full responsibility for the content of the publication.

Declaration of interests

The authors declare the following financial interests/personal relationships which may be considered as potential competing interests:

Mostafa Zarandi reports financial support was provided by Horizon 2020 European Innovation Council Fast Track to Innovation. MOSTAFA ZARANDI reports financial support was provided by Rovira i Virgili University. Laureano Jimenez reports financial support was provided by Spanish Ministry of Science and Innovation. Angel Galan-Martin reports was provided by Spanish Ministry of Science, Innovation. Mostafa Zarandi reports a relationship with Horizon 2020 European Innovation Council Fast Track to Innovation that includes: funding grants. If there are other authors, they declare that they have no known competing financial interests or personal relationships that could have appeared to influence the work reported in this paper.

Acknowledgments

This project has received funding from the European Union's Horizon 2020 research and innovation program under the Marie Skłodowska-Curie grant agreement No. 945413 and from the Universitat Rovira i Virgili (URV). The URV authors would like to thank the Spanish Ministry of Science and Innovation (PID2021-127713OA-I00 and PID2021-124139NB-C22). Ángel Galán-Martín thanks the Spanish Ministry of Science, Innovation, and Universities for the financial support through the "Beatriz Galindo" Program (BG20/00074).

Appendix A. Supplementary data

Supplementary data to this article can be found online at https://doi.org/10.1016/j.ijhydene.2025.01.290.

References

[1] Tryggestad C, Sharma N, Rolser O, Smeets B, Wilthaner M, van de Staaij J, Gruenewald T, Noffsinger J, Tiemersma L. Global Energy Perspective 2022: Executive summary. New York: McKinsey & Company; 2022. Available at, https://www.mckinsey.com/%7E/media/McKinsey/Industries/Oil%20and%20Gas/Our%20Insights/Global%20Energy%20Perspective%202022/Global-Energy-Perspective-2022-Executive-Summary.pdf [Accessed 28 February 2024].

[2] Bouckaert S, Pales AF, McGlade C, Remme U, Wanner B, Varro L, et al. Net zero by 2050: a roadmap for the global energy sector. 2021.

[3] Steynberg AP. Introduction to fischer-tropsch technology. Stud Surf Sci Catal 2004; 152:1–63. https://doi.org/10.1016/S0167-2991(04)80458-0. Elsevier.

[4] Faizan M, Song H. Critical review on catalytic biomass gasification: state-of-Art progress, technical challenges, and perspectives in future development. J Clean Prod 2023;408:137224. https://doi.org/10.1016/j.jclepro.2023.137224.

[5] Santos RG dos, Alencar AC. Biomass-derived syngas production via gasification process and its catalytic conversion into fuels by Fischer Tropsch synthesis: a review. Int J Hydrogen Energy 2020;45:18114–32. https://doi.org/10.1016/j.ijhydene.2019.07.133.

[6] Ren J, Cao JP, Zhao XY, Yang FL, Wei XY. Recent advances in syngas production from biomass catalytic gasification: a critical review on reactors, catalysts, catalytic mechanisms and mathematical models. Renew Sustain Energy Rev 2019;116: 109426. https://doi.org/10.1016/J.RSER.2019.109426.

[7] Ail SS, Dasappa S. Biomass to liquid transportation fuel via Fischer Tropsch synthesis - technology review and current scenario. Renew Sustain Energy Rev 2016;58:267–86. https://doi.org/10.1016/j.rser.2015.12.143.

[8] Chiodini A, Bua L, Carnelli L, Zwart R, Vreugdenhil B, Vocciante M. Enhancements in Biomass-to-Liquid processes: gasification aiming at high hydrogen/carbon monoxide ratios for direct Fischer-Tropsch synthesis applications. Biomass Bioenergy 2017;106:104–14. https://doi.org/10.1016/j.biombioe.2017.08.022.

[9] Zarandi M, Panahi M, Rafiee A. Simulation of a natural gas-to-liquid process with a multitubular fischer-tropsch reactor and variable chain growth factor for product

distribution. Ind Eng Chem Res 2020;59. https://doi.org/10.1021/acs.iecr.0c01951.
[10] Choudhury HA, Chakma S, Moholkar VS. Chapter 14 - biomass gasification integrated fischer-tropsch synthesis: perspectives, opportunities and challenges. In: Pandey A, Bhaskar T, Stöcker M, Sukumaran RK, editors. Recent advances in thermo-chemical conversion of biomass. Boston: Elsevier; 2015. p. 383–435. https://doi.org/10.1016/B978-0-444-63289-0.00014-4.
[11] Bimbela F, Oliva M, Ruiz J, García L, Arauzo J. Hydrogen production via catalytic steam reforming of the aqueous fraction of bio-oil using nickel-based coprecipitated catalysts. Int J Hydrogen Energy 2013;38:14476–87. https://doi.org/10.1016/j.ijhydene.2013.09.038.
[12] Mandal S, Daggupati S, Majhi S, Thakur S, Bandyopadhyay R, Das AK. Catalytic gasification of biomass in dual-bed gasifier for producing tar-free syngas. Energy Fuel 2019;33:2453–66. https://doi.org/10.1021/acs.energyfuels.8b04305.
[13] Li Z, Xu H, Yang W, Xu M, Zhao F. Numerical investigation and thermodynamic analysis of syngas production through chemical looping gasification using biomass as fuel. Fuel 2019;246:466–75. https://doi.org/10.1016/j.fuel.2019.03.007.
[14] Gil-Lalaguna N, Sánchez JL, Murillo MB, Rodríguez E, Gea G. Air-steam gasification of sewage sludge in a fluidized bed. Influence of some operating conditions. Chem Eng J 2014;248:373–82. https://doi.org/10.1016/j.cej.2014.03.055.
[15] Shen Y. Biomass pretreatment for steam gasification toward H2-rich syngas production – an overview. Int J Hydrogen Energy 2024;66:90–102. https://doi.org/10.1016/j.ijhydene.2024.04.096.
[16] Shen Y, Liu Y, Yu H. Enhancement of the quality of syngas from catalytic steam gasification of biomass by the addition of methane/model biogas. Int J Hydrogen Energy 2018;43:20428–37. https://doi.org/10.1016/j.ijhydene.2018.09.068.
[17] Lalsare A, Wang Y, Li Q, Sivri A, Vukmanovich RJ, Dumitrescu CE, et al. Hydrogen-rich syngas production through synergistic methane-activated catalytic biomass gasification. ACS Sustain Chem Eng 2019;7. https://doi.org/10.1021/acssuschemeng.9b02663.
[18] Dong Y, Steinberg M. Hynol - an economical process for methanol production from biomass and natural gas with reduced CO2 emission. Int J Hydrogen Energy 1997;22. https://doi.org/10.1016/s0360-3199(96)00198-x.
[19] Borgwardt RH. Biomass and natural gas as co-feedstocks for production of fuel for fuel-cell vehicles. Biomass Bioenergy 1997;12. https://doi.org/10.1016/S0961-9534(97)87131-0.
[20] Li H, Hong H, Jin H, Cai R. Analysis of a feasible polygeneration system for power and methanol production taking natural gas and biomass as materials. Appl Energy 2010;87. https://doi.org/10.1016/j.apenergy.2009.07.001.
[21] Gardezi SA, Joseph B, Prado F, Barbosa A. Thermochemical biomass to liquid (BTL) process: bench-scale experimental results and projected process economics of a commercial scale process. Biomass Bioenergy 2013;59:168–86. https://doi.org/10.1016/j.biombioe.2013.09.010.
[22] Seifkar N, Lu X, Withers M, Malina R, Field R, Barrett S, et al. Biomass to liquid fuels pathways: a techno-economic environmental evaluation. 2015.
[23] Liu G, Williams RH, Larson ED, Kreutz TG. Design/economics of low-carbon power generation from natural gas and biomass with synthetic fuels co-production. Energy Proc 2011;4:1989–96. https://doi.org/10.1016/J.EGYPRO.2011.02.080.
[24] Baliban RC, Elia JA, Floudas CA. Biomass and natural gas to liquid transportation fuels: process synthesis, global optimization, and topology analysis. Ind Eng Chem Res 2013;52:3381–406. https://doi.org/10.1021/IE3024643.
[25] Hailey AK, Meerman JC, Larson ED, Loo YL. Low-carbon "drop-in replacement" transportation fuels from non-food biomass and natural gas. Appl Energy 2016;183:1722–30. https://doi.org/10.1016/J.APENERGY.2016.09.068.
[26] Wright MM, Seifkar N, Green WH, Román-Leshkov Y. Natural gas and cellulosic biomass: a clean fuel combination? Determining the natural gas blending wall in biofuel production. Environ Sci Technol 2015;49:8183–92. https://doi.org/10.1021/ACS.EST.5B00060.
[27] Zhang Y, Sahir AH, Tan ECD, Talmadge MS, Davis R, Biddy MJ, et al. Economic and environmental potentials for natural gas to enhance biomass-to-liquid fuels technologies. Green Chem 2018;20:5358–73. https://doi.org/10.1039/C8GC01257A.
[28] Panahi M, Rafiee A, Skogestad S, Hillestad M. A natural gas to liquids process model for optimal operation. Ind Eng Chem Res 2011;51:425–33. https://doi.org/10.1021/IE2014058.
[29] Mokheimer EMA, Hussain MI, Ahmed S, Habib MA, Al-Qutub AA. On the modeling of steam methane reforming. Journal of Energy Resources Technology, Transactions of the ASME 2015;137. https://doi.org/10.1115/1.4027962/443346.
[30] Puig-Gamero M, Pio DT, Tarelho LAC, Sánchez P, Sanchez-Silva L. Simulation of biomass gasification in bubbling fluidized bed reactor using aspen plus. Energy Convers Manag 2021;235:113981. https://doi.org/10.1016/J.ENCONMAN.2021.113981.
[31] Steynberg AP, Dry ME, Davis BH, Breman BB. Fischer-tropsch reactors, vol. 152. Elsevier; 2004. https://doi.org/10.1016/S0167-2991(04)80459-2.
[32] AlNouss A, McKay G, Al-Ansari T. Enhancing waste to hydrogen production through biomass feedstock blending: a techno-economic-environmental evaluation. Appl Energy 2020;266:114885. https://doi.org/10.1016/j.apenergy.2020.114885.
[33] Tezer Ö, Karabağ N, Öngen A, Çolpan CÖ, Ayol A. Biomass gasification for sustainable energy production: a review. Int J Hydrogen Energy 2022;47:15419–33. https://doi.org/10.1016/j.ijhydene.2022.02.158.
[34] Salkuyeh YK, Saville BA, MacLean HL. Techno-economic analysis and life cycle assessment of hydrogen production from different biomass gasification processes. Int J Hydrogen Energy 2018;43:9514–28. https://doi.org/10.1016/j.ijhydene.2018.04.024.
[35] Pala LPR, Wang Q, Kolb G, Hessel V. Steam gasification of biomass with subsequent syngas adjustment using shift reaction for syngas production: an Aspen Plus model. Renew Energy 2017;101:484–92. https://doi.org/10.1016/J.RENENE.2016.08.069.
[36] Al-Zareer M, Dincer I, Rosen MA. Influence of selected gasification parameters on syngas composition from biomass gasification. Journal of Energy Resources Technology, Transactions of the ASME 2018;140. https://doi.org/10.1115/1.4039601/367454.
[37] De Lasa H, Salaices E, Mazumder J, Lucky R. Catalytic steam gasification of biomass: catalysts, thermodynamics and kinetics. Chem Rev 2011;111:5404–33. https://doi.org/10.1021/CR200024W.
[38] Chang ACC, Chang H-F, Lin F-J, Lin K-H, Chen C-H. Biomass gasification for hydrogen production. Int J Hydrogen Energy 2011;36:14252–60. https://doi.org/10.1016/j.ijhydene.2011.05.105.
[39] Al-Zareer M, Dincer I, Rosen MA. Effects of various gasification parameters and operating conditions on syngas and hydrogen production. Chem Eng Res Des 2016;115:1–18. https://doi.org/10.1016/j.cherd.2016.09.009.
[40] Xu J, Froment GF. Methane steam reforming, methanation and water-gas shift: I. Intrinsic kinetics. AIChE J 1989;35:88–96. https://doi.org/10.1002/AIC.690350109.
[41] Antonini C, Pérez-Calvo J-F, van der Spek M, Mazzotti M. Optimal design of an MDEA CO2 capture plant for low-carbon hydrogen production — a rigorous process optimization approach. Sep Purif Technol 2021;279:119715. https://doi.org/10.1016/j.seppur.2021.119715.
[42] Shirmohammadi R, Aslani A, Batuecas E, Ghasempour R, Romeo LM, Petrakopoulou F. A comparative life cycle assessment for solar integration in CO2 capture utilized in a downstream urea synthesis plant. J CO2 Util 2023;74:102534. https://doi.org/10.1016/j.jcou.2023.102534.
[43] Taherzadeh M, Tahouni N, Panjeshahi MH. Design of an integrated system for electrofuels production through Fischer-tropsch process. Int J Hydrogen Energy 2024. https://doi.org/10.1016/j.ijhydene.2024.03.067.
[44] Sonal Ahmad E, Upadhyayula S, Pant KK. Biomass-derived CO2 rich syngas conversion to higher hydrocarbon via Fischer-Tropsch process over Fe–Co bimetallic catalyst. Int J Hydrogen Energy 2019;44:27741–8. https://doi.org/10.1016/j.ijhydene.2019.09.015.
[45] Atashi H, Rezaeian F. Modelling and optimization of Fischer–Tropsch products through iron catalyst in fixed-bed reactor. Int J Hydrogen Energy 2017;42:15497–506. https://doi.org/10.1016/j.ijhydene.2017.04.224.
[46] Abdelouahed L, Authier O, Mauviel G, Corriou JP, Verdier G, Dufour A. Detailed modeling of biomass gasification in dual fluidized bed reactors under aspen plus. Energy & Fuels 2012;26:3840–55. https://doi.org/10.1021/ef300411k.
[47] Atashi H, Rezaeian F. Modelling and optimization of Fischer–Tropsch products through iron catalyst in fixed-bed reactor. Int J Hydrogen Energy 2017;42:15497–506. https://doi.org/10.1016/j.ijhydene.2017.04.224.
[48] Peters MS, Timmerhaus KD, West RE. Plant design and economics for chemical engineers. fifth ed. New York: McGraw-Hill International Book; 2003.
[49] ISO 14040. Environmental management—life cycle assessment—principles and framework. 2006. p. 235–48.
[50] Huijbregts MAJ, Steinmann ZJN, Elshout PMF, Stam G, Verones F, Vieira M, et al. ReCiPe2016: a harmonised life cycle impact assessment method at midpoint and endpoint level. Int J Life Cycle Assess 2017;22:138–47. https://doi.org/10.1007/S11367-016-1246-Y.
[51] Cabrera-Jiménez R, Mateo-Sanz JM, Gavaldà J, Jiménez L, Pozo C. Comparing biofuels through the lens of sustainability: a data envelopment analysis approach. Appl Energy 2022;307:118201. https://doi.org/10.1016/j.apenergy.2021.118201.
[52] Norouzi M, Colclough S, Jiménez L, Gavaldà J, Boer D. Low-energy buildings in combination with grid decarbonization, life cycle assessment of passive house buildings in Northern Ireland. Energy Build 2022;261:111936. https://doi.org/10.1016/j.enbuild.2022.111936.
[53] von der Assen N, Jung J, Bardow A. Life-cycle assessment of carbon dioxide capture and utilization: avoiding the pitfalls. Energy Environ Sci 2013;6:2721–34. https://doi.org/10.1039/C3EE41151F.
[54] Norouzi M, Haddad AN, Jiménez L, Hoseinzadeh S, Boer D. Carbon footprint of low-energy buildings in the United Kingdom: effects of mitigating technological pathways and decarbonization strategies. Sci Total Environ 2023;882:163490. https://doi.org/10.1016/j.scitotenv.2023.163490.
[55] Wang M, Elgowainy A, Lee U, Bafana A, Banerjee S, Benavides P, et al. Greenhouse gases, regulated emissions, and energy use in technologies model (2021 Excel). Argonne, IL (United States): Argonne National Laboratory (ANL); 2021.
[56] Tijmensen MJA, Faaij APC, Hamelinck CN, van Hardeveld MRM. Exploration of the possibilities for production of Fischer Tropsch liquids and power via biomass gasification. Biomass Bioenergy 2002;23:129–52. https://doi.org/10.1016/S0961-9534(02)00037-5.